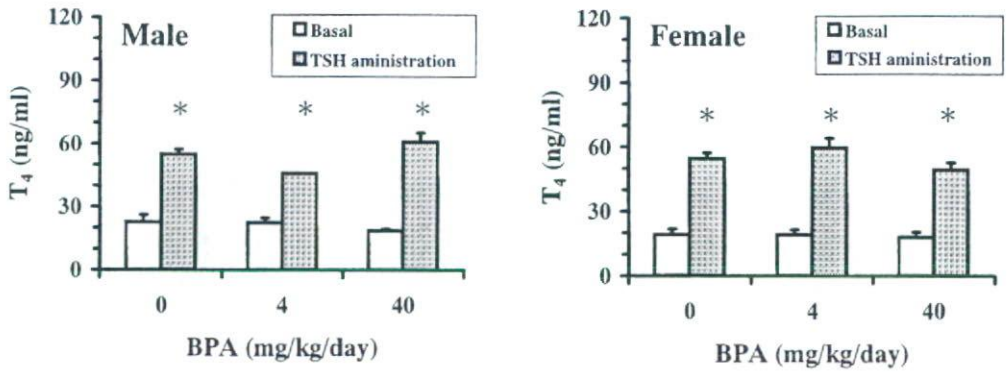

Fig. 2. Effects of maternal exposure to BPA on T_4 response to TSH in male and female offspring at 9 weeks of age.
Each column and vertical bar represents the mean and SEM, respectively. *Significantly different from the corresponding basal value ($p<0.05$).

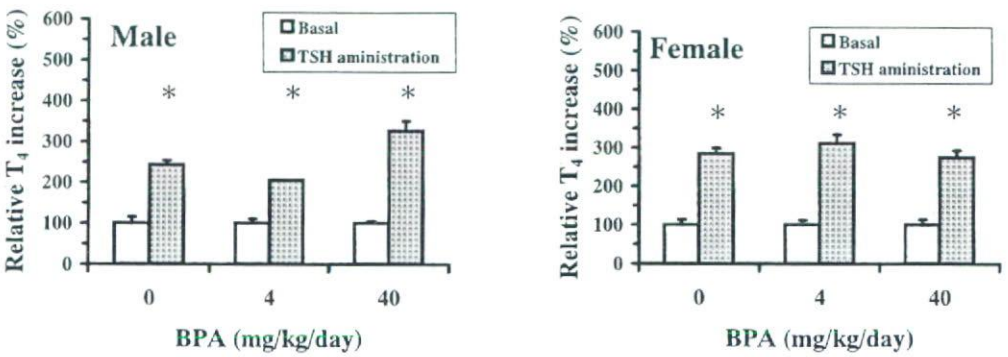

Fig. 3. Effects of maternal exposure to BPA on relative T_4 increase in response to TSH in male and female offspring at 9 weeks of age.
Each column and vertical bar represents the mean and SEM, respectively. *Significantly different from the corresponding basal value ($p<0.05$).

fetal and early neonatal periods, impaired thyroid hormone function may affect somatic growth[20]. BPA may act as an agonist or antagonist of the thyroid hormone receptor because of its structural similarity to thyroid hormone. Hence, given that thyroid hormone receptors are expressed ubiquitously and abundantly in various organs, BPA may perturb thyroid hormone action throughout the body tissue. Furthermore, BPA was observed to distribute rapidly in fetuses via placental transfer after a single BPA administration to pregnant female rats[21], mice and monkeys[22]; i.e., the placental barrier cannot block BPA transfer. Despite this high transplacental passage, there is sufficient glucuronyl transferase activity to metabolize BPA to BPA-monoglucuronide even in neonatal rats[23]. Although BPA may have the potential to disrupt thyroid hormone action through the thyroid hormone receptor, the results of this study confirmed that thyroid status was unaffected after *in utero* and lactational exposures of the offspring to BPA. The fact that normal somatic growth is observed in rat offspring following exposure of dams to BPA (even at high doses) [16] has led to the conclusion that the thyroid remains intact in the offspring.

In vitro studies have demonstrated the binding of BPA to the thyroid hormone receptor. Kitamura *et al.* reported that BPA does not inhibit the binding of T_3 to the thyroid hormone receptor and does not inhibit the hormonal activity of T_3 to induce growth and GH production of the rat pituitary cell line GH3[15]. On the other hand, Moriyama *et al.* used a competitive binding assay to confirm that BPA binds weakly to thyroid hormone receptors in rat liver nuclear extract[14]. Furthermore, BPA was shown to suppress T_3-stimulated transcriptional activity in transient expression assays[14]. The discrepancies between these *in vitro* studies indicate that further investigation is required to clarify the possible mechanism(s) of BPA action on the thyroid hormone receptor. Our results here are in accordance with an *in vitro* study reported by Kitamura *et al.*[15], however, we have no plausible

explanation for the differences between these *in vitro* studies and the *in vivo* outcome that we describe here.

In conclusion, the results of the present study suggest that *in utero* and lactational exposure to BPA does not have an effect on thyroid status in the F_1 generation of male and female rats under our experimental conditions.

Acknowledgments

We thank Mr. T. Murase (Animal Care, Inc., Tokyo, Japan) for his continuous support and valuable advice. This study was conducted as a part of the contract research with the Ministry of Health, Labour and Welfare, which was supported by funds from the Ministry of the Environment.

References

1) Brotons JA, Olea-Serrano MF, Villalobos M, Pedraza V, Olea N (1995) Xenoestrogens released from lacquer coatings in food cans. Environ Health Perspect **103**, 608-12.
2) Olea N, Pulgar R, Perez P, Olea-Serrano F, Rivas A, Novillo-Fertrell A, Pedraza V, Soto AM, Sonnenschein C (1996) Estrogenicity of resin-based composites and sealants used in dentistry. Environ Health Perspect **104**, 298–305.
3) Krishnan AV, Stathis P, Permuth SF, Tokes L, Feldman D (1993) Bisphenol-A: an estrogenic substance is released from polycarbonate flasks during autoclaving. Endocrinology **132**, 2279–86.
4) Scientific Committee on Food (2002) Opinion of the Scientific Committee on Food on Bisphenol A, April 17, http://europa.eu.int/comm/food/fs/sc/scf/out128_en.pdf.
5) Nagel SC, vom Saal FS, Thayer KA, Dhar MG, Boechler M, Welshons WV (1997) Relative binding affinity-serum modified access (RBA-SMA) assay predicts the relative *in vivo* bioactivity of the xenoestrogens bisphenol A and octylphenol. Environ Health Perspect **105**, 70–6.
6) vom Saal FS, Cooke PS, Buchanan DL, Palanza P, Thayer KA, Nagel SC, Parmigiani S, Welshons WV (1998) A physiologically based approach to the study of bisphenol A and other estrogenic chemicals on the size reproductive organs, daily sperm production, and behavior. Toxicol Ind Health **14**, 239–60.
7) Ashby J, Tinwell H, Haseman J (1999) Lack of effects for low dose levels of bisphenol A and diethylstilbestrol on the prostate gland of CF1 mice exposed *in utero*. Regul Toxicol Pharmacol **30**, 156–66.
8) Cagen SZ, Waechter JM Jr, Dimond SS, Breslin WJ, Butala JH, Jekat FW, Joiner RL, Shiotsuka RN, Veenstra GE, Harris LR (1999) Normal reproductive organ development in CF-1 mice following prenatal exposure to bisphenol A. Toxicol Sci **50**, 36–44.
9) Cagen SZ, Waechter JM Jr, Dimond SS, Breslin WJ, Butala JH, Jekat FW, Joiner RL, Shiotsuka RN, Veenstra GE, Harris LR (1999) Normal reproductive organ development in Wistar rats exposed to bisphenol A in the drinking water. Regul Toxicol Pharmacol **30**, 130–9.
10) Ema M, Fujii S, Fukuhara M, Kiguchi M, Ikka T, Harazono A (2001) Rat two-generation reproductive toxicity study of bisphenol A. Reprod Toxcol **15**, 505–23.
11) Tyl RW, Myers CB, Marr MC, Thomas BF, Keimowitz AR, Brine DR, Veselica MM, Fail PA, Chang TY, Seely JC, Joiner RL, Butala JH, Dimond SS, Cagen SZ, Shiotsuka RN, Stropp GD, Waechter JM (2002) Three-generation reproductive toxicity study of dietary bisphenol A in CD Sprague-Dawley rats. Toxicol Sci **68**, 121–46.
12) Dodds EC, Lawson W (1936) Synthetic estrogenic agents without the phenanthrene nucleus. Nature **137**, 996.
13) Gaido KW, Leonard LS, Lovell S, Gould JC, Babai D, Portier CJ, McDonnell DP (1997) Evaluation of chemicals with endocrine modulating activity in a yeast-based steroid hormone receptor gene transcription assay. Toxicol Appl Pharmacol **143**, 205–12.
14) Moriyama K, Tagami T, Akamizu T, Usui T, Saijo M, Kanamoto N, Hataya Y, Shimatsu A, Kuzuya H, Nakao K (2002) Thyroid hormone action is disrupted by bisphenol A as an antagonist. J Clin Endocrinol Metab **87**, 5185–90.
15) Kitamura S, Jinno N, Ohta S, Kuroki H, Fujimoto N (2002) Thyroid hormonal activity of the flame retardants tetrabromobisphenol A and tetrachlorobisphenol A. Biochem Biophys Res Commun **293**, 554–9.
16) Kobayashi K, Miyagawa M, Wang RS, Sekiguchi S, Suda M, Honma T (2002) Effects of *in utero* and lactational exposure to bisphenol A on somatic growth and anogenital distance in F_1 rat offspring. Ind Health **40**, 375–81.
17) Morrissey RE, George JD, Price CJ, Tyl RW, Marr MC, Kimmel CA (1987) The developmental toxicity of bisphenol A in rats and mice. Fundam Appl Toxicol **8**, 571–82.

18) Kwon S, Stedman DB, Elswick RC, Cattey RC, Welsch F (2000) Pubertal development and reproductive functions of Crl: CD BR Sprague-Dawley rats exposed to bisphenol A during prenatal and postnatal development. Toxicol Sci **55**, 399–406.
19) Watanabe S, Wang RS, Miyagawa M, Kobayashi K, Suda M, Sekiguchi S, Honma T (2003) Imbalance of testosterone level in male offspring of rats perinatally exposed to bisphenol A. Ind Health **41**, 335–41.
20) Griffin JE (1996) The thyroid. Textbook of Endocrine Physiology Third ed., eds. by Griffin JE, Ojeda SR, 260–83, Oxford University Press, New York.
21) Takahashi O, Oishi S (2000) Disposition of orally administered 2, 2-Bis (4-hydroxyphenyl) propane (Bisphenol A) in pregnant rats and the placental transfer to fetuses. Environ Health Perspect **108**, 931–5.
22) Uchida K, Suzuki A, Kobayashi Y, Buchanan DL, Sato T, Watanabe H, Katsu J, Suzuki J, Asaoka C, Mori C, Arizono K, Iguchi T (2002) Bisphenol-A administration during pregnancy results in fetal exposure in mice and monkeys. J Health Sci **48**, 579–82.
23) Domoradzki JY, Thornton CM, Pottenger LH, Hansen SC, Card TL, Markham DA, Dryzga MD, Shiotsuka RN, Waechter JM Jr (2004) Age and dose dependency of the pharmacokinetics and metabolism of bisphenol A in neonatal Sprague-Dawley rats following oral administration. Toxicol Sci **77**, 230–42.

Dear Dr.Noji:

Manuscript number: GT-2007-00392R
Title: Atelocollagen-mediated local and systemic applications of myostatin-targeting siRNA increase skeletal muscle mass
Corresponding Author:Prof. Noji

I am delighted to tell you that your above mentioned manuscript has been accepted for publication in Gene Therapy.

Please see below a link to the licence to publish form for the Journal. If you have not already done so, please fax the completed form for the attention of Paola Grandi to: +1 412 624 8997

http://mts-gt.nature.com/letters/gt_copyright.pdf

If your paper contains colour artwork, please click the link below and complete the Color Authorisation Form. This form must be faxed back along with your Licence to Publish form.

http://mts-gt.nature.com/letters/gt_color.pdf

Your paper cannot be processed until we have received both of these forms.

You will receive galley proofs directly from the publisher. Please review the proofs and return them promptly to the publisher.

Thank you for submitting this work to Gene Therapy.

Yours sincerely

Joseph Glorioso, Ph.D.
Editor, Gene Therapy

Atelocollagen-mediated local and systemic applications of myostatin-targeting siRNA increase skeletal muscle mass

Nao Kinouchi 1, Yutaka Ohsawa 2, Naozumi Ishimaru 3, Hideyo Ohuchi 4*, Yoshihide Sunada 2, Yoshio Hayashi 3, Yukiho Tanimoto 1, Keiji Moriyama 1, 5 and Sumihare Noji 4*

1 Department of Orthodontics and Dentofacial Orthopedics, Graduate School of Dentistry, The University of Tokushima, 3-18-15 Kuramoto, Tokushima 770-8504, Japan;

2 Division of Neurology, Department of Internal Medicine, Kawasaki Medical School, 577 Matsushima, Kurashiki City, Okayama 701-0192, Japan;

3 Department of Oral Molecular Pathology, Institute of Health Bioscience, The University of Tokushima Graduate School, 3-18-15 Kuramoto, Tokushima 770-8504, Japan;

4 Department of Life Systems, Institute of Technology and Science, The University of Tokushima, 2-1 Minami-Jyosanjima-cho, Tokushima 770-8506, Japan.

5 Present address: Department of Maxillofacial Orthognathics, Graduate School, Tokyo Medical and Dental University, 1-5-45 Yushima, Bunkyo-ku, Tokyo 113-8549, Japan

* Correspondence should be addressed to H.O. or S.N.

Keywords: siRNA, atelocollagen, myostatin, muscle atrophy

RNA interference (RNAi) offers a novel therapeutic strategy based on the highly specific and efficient silencing of a target gene[1-4]. Since it relies on small interfering RNAs (siRNAs), which are the mediators of RNAi-induced specific mRNA degradation[2], a major issue is the delivery of therapeutically active siRNAs into the target tissue/target cells in vivo[3,4]. For safety reasons, strategies based on vector delivery may be of only limited clinical use. The more desirable approach is to directly apply active siRNAs in vivo. Here, we report the effectiveness of in vivo siRNA delivery into skeletal muscles of normal or diseased mice through nano-particle formation of chemically unmodified siRNAs with atelocollagen (ATCOL)[5-7]. ATCOL-mediated local application of siRNA targeting myostatin (growth/differentiation factor 8, GDF8), a negative regulator of skeletal muscle growth[8], in mouse skeletal muscles or intravenously, caused a marked increase in the muscle mass within a few weeks after application. These results imply that ATCOL-mediated application of siRNAs is a powerful tool for future therapeutic use for genetic diseases including muscular atrophy.

Skeletal muscles are the crucial morpho-functional organs, and their atrophy causes severe conditions for life such as muscular dystrophies. Duchenne muscular dystrophy (DMD), for instance, is a severe muscle wasting disorder affecting 1/3500 male birth[9]. There is currently no effective treatment, but gene therapy approaches are offering viable avenues for treatment development[10]. As one of therapeutic approaches, inhibition of myostatin by using anti-myostatin blocking antibodies has been employed to increase muscle mass[11]. However, generating antibodies against recombinant target proteins is time-consuming and requires a lord of efforts. Recently, we demonstrated that inhibition of myostatin by overexpression of the myostatin pro-domain[12] prevented muscular atrophy and normalized intracellular myostatin signaling in the model mice for limb-girdle muscular dystrophy 1C (LGMD1C)[13]. On the other hand, Magee et al.[14] demonstrated that down-regulation of myostatin expression by transduction of a plasmid expressing a short hairpin interfering RNA (shRNA) against myostatin using electroporation can increase local skeletal muscle mass. For safety reasons, however, strategies based on vector delivery may be of only limited clinical use. The more desirable approach is to directly apply active short interfering RNAs (siRNAs) in vivo. As one of the practical platforms for siRNA delivery, we sought to employ an

atelocollagen-mediated oligonucleotide delivery system to apply myostatin-targeting siRNA into muscles.

We utilized the siRNA-sequences reported previously[13,14] (GDF8 siRNA26, 5'-AAGATGACGATTATCACGCTA-3', position 426-446). It has been noted that this sequence can target myostatin mRNA not only of mouse but also human, rat, rabbit, cow, macaque, and baboon, based on Blast search (NCBI). To confirm the silencing effect of this siRNA, we constructed a plasmid of pSilencer 2.1-U6 neo containing the target sequence and transfected the plasmid into a mouse myoblast cell line, C2C12 cells, which had been made forced to stably-express myostatin. We confirmed that the RNAi-construct could effectively down-regulate the expression of myostatin in the C2C12 cells (see Supplementary Figures online).

After forming the nano-particle complex containing the GDF8 siRNA26 (10 μM) and atelocollagen (ATCOL), we injected the GDF8 siRNA26-atelocollagen (Mst-siRNA/ATCOL) complex into the masseter and biceps femoris muscles of 20-week old C57BL/6 mice. As a control, we injected control scrambled siRNAs/ATCOL complex in the contralateral muscles. Two weeks after injection, we observed gross morphology of the muscles and dissected the muscle tissues. After injection of the Mst-siRNA/ATCOL complex, both muscles (on the left side) were enlarged, while no significant change was observed on the contralateral side (Fig. 1a). We also measured the muscle weight, finding that the Mst-siRNA/ATCOL-treated muscles weighed significantly more than those on the control side (Fig. 1b). The Mst-siRNA/ATCOL-treated muscles were further examined by Western blot analysis for myostatin, showing the decreased expression of myostatin on the treated side (Fig. 1c). Histological analysis has shown that the myofibril sizes of the masseter muscles treated with the Mst-siRNA/ATCOL complex were larger than those of the control (Fig. 2a). Examining the sizes of 200 myofibers per each group, the population of myofibril sizes indicated a shift from smaller to larger fibers in the Mst-siRNA/ATCOL-treated muscle (Fig. 2b). The average myofibril size of the muscle treated with Mst-siRNA/ATCOL gained approximately 1.3 times more than that of control (Fig. 2b). In the meanwhile, we did not observe any general sign of ill health and deaths during the period of experiment. These results indicate that the increase of the Mst-siRNA/ATCOL-treated muscle mass is caused by their hypertrophy.

We next questioned whether this effect of hypertrophy after local injection of the Mst-siRNA/ATCOL complex observed in normal mice was relevant to dystrophin deficient *mdx* mouse, an animal model for DMD[9,16]. We intramuscularly injected the same Mst-siRNA/ATCOL complex into the masseter and tibial muscles on the left side of 20-week-old *mdx* male mice. Within two weeks after the single injection, a dramatically increased muscle mass was observed in the Mst-siRNA/ATCOL-treated muscle (Fig. 3a). Western blot analysis has shown that the protein levels of myostatin in the muscles treated with the Mst-siRNA/ATCOL complex were significantly decreased, but not in the contralateral muscles treated with control siRNAs/ATCOL complex (Fig. 3b). Furthermore, immunohistochemical analysis on the masseter using an anti-laminin α2 antibody has shown an increase in the mean myofiber size of the Mst-siRNA/ATCOL-treated muscle (Fig. 3c), as is the case for the wild-type (not shown). Based on these results, it seems that myostatin maintains satellite cells or muscle stem cells in a quiescent state. Reduced myostatin activity would lead to activation of these cells and fusion into existing fibers, leading to fiber hypertrophy as proposed previously[15].

Atelocollagen has been also used for systemic siRNA-delivery into cancer metastasis animal models or to silence the exogenous genes as luciferase[7]. We therefore examined whether systemic administration of the Mst-siRNA/ATCOL complex would have an effect on silencing the myostatin expression and muscle enlargement. Strikingly, we observed a significant increase in muscle weight and fiber size within three weeks (Fig. 4), showing the first time that the siRNA/atelocollagen complex would be a useful tool for systemic siRNA-delivery that will be promising for a therapeutic remedy against systemic diseases of muscles, bones, blood, and the immune system.

We have shown that local and systemic applications of siRNA against myostatin coupled with atelocollagen markedly stimulate the growth of muscles in vivo within a few weeks. The precise mechanisms by which atelocollagen achieves this effect has not been fully elucidated but it is thought that nuclease activity to siRNA may be prevented by atelocollagen[6]. As a single administration of siRNA/ATCOL against myostatin had a continuous muscle stimulative effect, this novel method of targeting

against muscle atrophy would be of considerable value for clinical applications.

Methods

Animals and administration of siRNA/atelocollagen complex

Histological and biochemical properties were analyzed with muscles from 20-week-old male C57BL/6 and *mdx* mice, as described previously[13]. Mst-siRNA or control scrambled siRNAs (final concentration was 10μM) were mixed with atelocollagen (AteloGene™, Kohken, Tokyo) according to the manufacturer's instructions. After anesthesia of the mice by Nembutal (25mg/kg i.p.), the Mst-siRNA/ATCOL complex was injected into the masseter and biceps femoris or tibial muscles. As a control, the control-siRNA/ATCOL complex was injected into the contralateral muscles on the right side. After 2 weeks, the muscles on both sides were harvested and processed for analysis. For systemic administration, the siRNA/ATCOL complex (40μM, 200 μl) was introduced intravenously via orbital veins at 4, 7, and 14 days after the first application (n=5). As a control, control scrambled siRNAs were injected into wild type male mice (20 weeks) (n=5). After 3 weeks, the quadriceps muscles on both sides were harvested and processed for analysis.

Histological analysis and immunohistochemistry

Muscles were fixed in 4% paraformaldehyde (PFA) /PBS at 4℃ overnight, dehydrated, and paraffin-embedded. Serial sections (5μm-thickness) were cut at mid-belly of muscle. Sections were examined after Hematoxylin and Eosin staining or labeling with anti-laminin α2-chain antibodies (4H8-2, Sigma). NIH Image (NIH, USA) software was used for morphometric measurements. AlexaFluor-594 conjugated anti-rat IgG antibodies (A-11007, Invitrogen) were used for immunohistochemistry.

Western blot analysis

Eighty micrograms of masseter muscle homogenates were resolved by SDS-PAGE and then transferred onto PDFV membranes for immunoblotting. After a blocking reaction (5% nonfat milk/1% BSA in PBS and 0.05% TritonX-100), the blots were incubated for 1hr at room temperature with mouse monoclonal anti-myostatin antibody (1:500; R&D systems) or anti-β–actin. After incubation with a secondary antibody (1:10000;

HRP-conjugated anti-rat antibody; Biosource International), the blots were developed using the ECL-plus kit (Amersham).

Statistical analysis

Student's t-test was used for determining statistical significance throughout the study. Graphical representation of data uses the following convention: mean ± S.D; treated muscles or mice in red; control muscles or mice in blue.

Note: Supplementary information is available.

ACKNOWLEDGEMENTS

We thank Drs. Shin-ichiro Nishimatsu, Tsutomu Nohno (Department of Molecular Biology, Kawasaki Medical School) for valuable advice. We also thank Shizuka Sasano (Division of Neurology, Kawasaki Medical School), Megumu Kita (Laboratory Animal Center, Kawasaki Medical School) for their technical assistances. This work was supported by a Research Grant (14B-4) for Nervous and Mental Disorders from the Ministry of Health, Labour and Welfare; a Grant (15131301) for Research on Psychiatric and Neurological Diseases and Mental Health from the Ministry of Health, Labour and Welfare of Japan and from JSPS KAKENHI (14370212) to SN, YO and YS; and by Research Project Grants (15-115B and 16-601) from Kawasaki Medical School to YO and YS.

AUTHOR CONTRIBUTIONS

NK, YO, NI, HO, YS, YH, KM, SN assisted in the design of the experiments. NK, YO and NI performed the experiments mainly for local and systemic application of siRNA and analyzed the data. NK and HO wrote the draft of the manuscript for the experimental sections, and HO and SN wrote the draft of the manuscript for the introduction and discussion sections. All authors contributed to the editing of the text. YS, OH and SN directed the overall project.

COMPETING INTERESTS STATEMENT

The authors declare no competing financial interests.

References

1. Fire, A., Xu, S., Montgomery, M.K., Kostas. S.A., Driver. S.E. & Mello CC. Potent and specific genetic interference by double-stranded RNA in *Caenorhabditis elegans*. *Nature* **391**, 806-811 (1998).

2. Elbashir, S.M., Harborth, J., Lendeckel, W., Yalcin, A., Weber, K. & Tuschl, T. Duplexes of 21-nucleotide RNAs mediate RNA interference in cultured mammalian cells. *Nature* **411**, 494-498 (2001).

3. Gary, D.J., Puri, N. & Won, Y.Y. Polymer-based siRNA delivery: perspectives on the fundamental and phenomenological distinctions from polymer-based DNA delivery. *J. Control Release* **121**, 64-73 (2007).

4. de Fougerolles, A., Vornlocher, H.P., Maraganore, J. & Lieberman, J. Interfering with disease: a progress report on siRNA-based therapeutics. *Nat. Rev. Drug Discov.* **6**, 443-453 (2007). Review.

5. Minakuchi, Y., Takeshita, F., Kosaka, N., Sasaki, H., Yamamoto, Y., Kouno, M., Honma, K., Nagahara, S., Hanai, K., Sano, A., Kato, T., Terada, M. & Ochiya, T. Atelocollagen-mediated synthetic small interfering RNA delivery for effective gene silencing in vitro and in vivo. *Nucleic Acids Res.* **32**, e109 (2004)

6. Takeshita, F., Minakuchi, Y., Nagahara, S., Honma, K., Sasaki, H., Hirai, K., Teratani, T., Namatame, N., Yamamoto, Y., Hanai, K., Kato, T., Sano, A. & Ochiya, T. Efficient delivery of small interfering RNA to bone-metastatic tumors by using atelocollagen *in vivo*. *Proc. Natl. Acad. Sci. U S A.* **102**, 12177-12182 (2005).

7. Takeshita, F. & Ochiya, T. Therapeutic potential of RNA interference against cancer. *Cancer Sci.* **97**, 689-696 (2006). Review.

8. McPherron, A.C., Lawler, A.M. & Lee, S.J. Regulation of skeletal muscle mass in mice by a new TGF-beta superfamily member. *Nature* **387**, 83-90 (1997).

9. Deconinck, N. & Dan, B. Pathophysiology of duchenne muscular dystrophy: current hypotheses. *Pediatr. Neurol.* **36**, 1-7 (2007). Review.

10. Foster, K., Foster, H. & Dickson, J.G. Gene therapy progress and prospects: Duchenne muscular dystrophy. *Gene Ther.* **13**, 1677-1685 (2006). Review.

11. Bogdanovich, S., Krag, T.O., Barton, E.R., Morris, L.D., Whittemore, L.A., Ahima, R.S. & Khurana, T.S. Functional improvement of dystrophic muscle by myostatin blockade. *Nature* **420**, 418-421 (2002).

12. Nishi, M., Yasue, A., Nishimatsu, S., Nohno, T., Yamaoka, T., Itakura, M., Moriyama, K., Ohuchi, H. & Noji, S. A missense mutant myostatin causes hyperplasia without hypertrophy in the mouse muscle. *Biochem. Biophys. Res. Commun.* **293**, 247-251 (2002).

13. Ohsawa, Y., Hagiwara, H., Nakatani, M., Yasue, A., Moriyama, K., Murakami, T., Tsuchida, K., Noji, S. & Sunada, Y. Muscular atrophy of caveolin-3-deficient mice is rescued by myostatin inhibition. *J. Clin. Invest.* **116**, 2924-2934 (2006).

14. Artaza, J.N., Bhasin, S., Magee, T.R., Reisz-Porszasz, S., Shen, R., Groome, N.P., Meerasahib, M.F. & Gonzalez-Cadavid, N.F. Myostatin inhibits myogenesis and promotes adipogenesis in C3H 10T(1/2) mesenchymal multipotent cells. *Endocrinology* **146**, 3547-3557 (2005).

15. Magee, T.R., Artaza, J.N., Ferrini, M.G., Vernet, D., Zuniga, F.I., Cantini, L., Reisz-Porszasz, S., Rajfer, J. & Gonzalez-Cadavid, N.F. Myostatin short interfering hairpin RNA gene transfer increases skeletal muscle mass. *J. Gene Med.* **8**, 1171-1181 (2006).

16. Bulfield, G., Siller W.G., Wight P.A. & Moore K.J. X chromosome-linked muscular dystrophy (mdx) in the mouse. *Proc. Natl. Acad. Sci. USA*. **81**, 1189–1192 (1984).

Figure legend

Figure 1 Local administration of the Mst-siRNA/ATCOL complex increases skeletal muscle mass in wild-type mice through inhibition of myostatin expression. (**a**) Photographs of muscles. Increased muscle mass were observed in the Mst-siRNA/ATCOL-treated (L) masseter (upper panels) and biceps femoris (lower panels), but not in the contralateral muscles (R). (**b**) Muscle weight. Mst-siRNA/ATCOL treated muscles had an increased weight significantly compared to those with control siRNA/ATCOL (masseter, 0.185 ± 0.041 versus 0.115 ± 0.019g; biceps, 0.307 ± 0.040 versus 0.232 ± 0.039g; $n=4$; $p < 0.05$). (**c**) Western blot analysis of the control and Mst-siRNA/ATCOL-treated masseter muscles, assessed at 2 weeks after single injection.

Figure 2 Muscle fiber size increases after inhibition of myostatin expression in the masseter muscle. (**a**) Hematoxylin-Eosin staining of the control (left) and Mst-siRNA/ATCOL treated masseter muscle (right). Scale bar: 50μm. (**b**) Distribution of myofibril sizes of the control (blue bars) and Mst-siRNA/ATCOL-treated (red bars) muscles. The right panel shows the average myofibril size (33.6 ± 1.5 versus 24.4 ± 1.1 μm; $n=200$; $p < 0.0001$).

Figure 3 Mst-siRNA/ATCOL treatment improves myofibril size in *mdx* mice. (**a**) Photographs of muscles. The leftward masseter (left and middle panels) and tibial (right panel) muscles injected with the Mst-siRNA/ATCOL complex intramuscularly show a marked increased muscle mass in 20-week-old *mdx* male mice. (**b**) Western blot analysis of the control and Mst-siRNA/ATCOL-treated masseter muscles, assessed at 2 weeks after single injection. Myostatin protein levels in the muscles injected with the Mst-siRNA/ATCOL complex are markedly decreased, but not in the contralateral muscles injected with the control-siRNA/ATCOL. (**c**) Immunohistochemical analysis of the cross-sectional myofiber area of the masseter muscle, with the anti-laminin α2 antibody, showing increased fiber size in the Mst-siRNA/ATCOL-treated (right panel) muscle, compared to that of control (left panel). Scale bar: 100μm.

Figure 4 Systemic administration of the Mst-siRNA/ATCOL complex induces muscle enlargement in the mouse through inhibition of myostatin expression. (**a**) Photographs of lower limbs from control (upper) and Mst-siRNA/ATCOL-treated (lower) mice. (**b**) Western blot analysis of the control and Mst-siRNA/ATCOL-treated muscles (quadriceps femoris), assessed at 3 weeks after triple injection. (**c**) Hematoxylin-Eosin staining of the control (left) and Mst-siRNA/ATCOL treated quadriceps muscle (right). Scale bar: 50μm. (**d**) Comparison of muscle weight/body weight index between the Mst-siRNA/ATCOL-treated mice and control-siRNA/ATCOL-treated mice (0.048 ± 0.002 versus 0.043 ± 0.001; $n=5$; $p < 0.01$). (**e**) Distribution of myofibril sizes of the control and Mst-siRNA/ATCOL-treated quadriceps muscles. The right panel shows the average myofibril size (33.92 ± 2.91 versus 22.95 ± 1.54 μm; $n=156$; $p < 0.01$).

Supplementary information

Methods

Cell culture

C2C12 cells obtained from ATCC were grown in DMEM supplemented with 20% fetal bovine serum (Sigma). To induce myoblast differentiation, C2C12 cells were grown in DMEM supplemented with 2% horse serum (Invitrogen).

RT-PCR analysis

Total RNA was extracted from cultured cells using Isogen (NipponGene, Japan) according to the manufacturer's instructions. One microgram of total RNA was reverse transcribed via priming with random 9mers. PCR was performed using one of the primer sets listed in Supplementary Table.

Plasmid construction and stable expression of myostatin

To generate a myostatin-expressing plasmid, a full-length cDNA of mouse myostatin was amplified using primers that contained the *BamH*I or *Apa*I sites. Primer sequences were the following: Forward ; 5'-CGGGATCCATGATGCAAAAACTGCAAATG-3'; Reverse ; 5'-GAAGGGCCCTGAGCACCCACAGCGGTCTACTACCAT-3'. After cleaving the appropriate restriction enzymes, the PCR products were subcloned into pcDNA3.1-myc/His A(Invitrogen), followed by sequencing. C2C12 cells (1×10^6) were transfected with 10μg of the myostatin-expressing plasmid (pcDNA3.1-Mst-myc) using Superfect Transfection Reagent (Qiagen). Stable myostatin-expressing clones were selected and maintained in 0.5mg/ml of G418 (Invitrogen).

Transient expression of shRNA plasmids

An shRNA-expressing plasmid targeted against mouse myostatin was constructed using pSilencer 2.1-U6 neo (Ambion) (pSi-Mst) according to the siRNA sequence previously published [13, 14]. COS-1 cells were transfected with pcDNA3.1-myc/His A and one of the following plasmids using Lipofectamine 2000 (Invitrogen): pSi-Mst, or control shRNA-expressing plasmid against green fluorescence protein, pSi-N (Ambion). Stable C2C12 cell lines expressing myostatin were transfected with pSi-Mst or pSi-N using Lipofectamine 2000.

Western blot analysis

Forty micrograms of cultured cell homogenates were resolved by SDS-PAGE and then transferred onto PDFV membranes for immunoblotting. After a blocking reaction (5% nonfat milk/1% BSA in PBS and 0.05% TritonX-100), the blots were incubated for 1hr at room temperature with one of the following antibodies: mouse monoclonal anti-myc antibody (1:1000; 9B11, Cell Signaling Technology), rabbit polyclonal anti-MyoD antibody (1:500; C-20: sc-304, Santa Cruz Biotechnology), rabbit polyclonal anti-pRb antibody (1:500; Ser795: sc-7986, Santa Cruz), mouse monoclonal anti-p53 antibody (1:500; DO-1: sc-126, Santa Cruz), or anti-β–actin. After incubation with a secondary antibody (1:10000; HRP-conjugated anti-mouse or anti-rabbit IgG), the blots were developed using the ECL-plus kit (Amersham).

Immunofluorescence

Parent and myostatin-expressing C2C12 cells were cultured on glass-bottomed dishes (MatTec Corporation). The stable C2C12 cells expressing myostatin were transfected with pSi-Mst or pSi-N using Lipofectamine 2000. At 24 hrs post transfection, immunofluorescence was performed according to standard protocols after fixation in 4% PFA/PBS using mouse monoclonal anti-myosin heavy chain (1:1000; Sigma) and FITC-conjugated anti-mouse IgG (Medical & Biological Laboratories).

Supplementary Table

Primer name	Sequence	Size (bp)	Annealing temp. (℃)
Myostatin Se	5'-CAGCCTGAATCCAACTTAGG-3'	167	58
Myostatin AS	5'-TCGCAGTCAAGCCCAAAGTC-3'		
MyoD Se	5'-GATGGCATGATGGATTACAGC-3'	528	64
MyoD AS	5'-GACTATGTCCTTTCTTTGGGG-3'		
Myogenin Se	5'-GCTCAGCTCCCTCAACCAG-3'	424	64
Myogenin AS	5'-ATGTGAATGGGGAGTGGGGA-3'		
p21 Se	5'-AATCCTGGTGATGTCCGACCTG-3'	158	64
p21 AS	5'-TCCGTGACGAAGTCAAAGTTCC-3'		
β-actin Se	5'-TTCTTTGCAGCTCCTTCGTTGCCG-3'	458	60
β-actin AS	5'-TGGATGGCTACGTACATGGCTGGG-3'		

Figure legend

Supplementary Figure The Mst-shRNA specifically regulates the expression of *myostatin* and its target genes in the C2C12 cells. (**a**) RT-PCR analysis of *myostatin* expression. Parental C2C12 cells do not express *myostatin*, whereas *myostatin* mRNA was detected in the stable C2C12 cell lines expressing pcDNA3.1-Mst-myc. After transfection of pSi-Mst into the C2C12/pcDNA 3.1-Mst-myc cells, expression of *myostatin* is down-regulated. (**b**) Western blot analysis of myc-tagged myostatin using anti-myc antibody. Parental and *myostatin*-expressing C2C12 cells were forced to differentiate in 2% horse serum and transfected with the plasmids indicated. Down-regulation of *myostatin* is observed for at least 3 days post transfection with pSi-Mst in the C2C12/pcDNA 3.1-Mst-myc cells. (**c**) RT-PCR analysis of *p21*, a target gene of myostatin. *p21* mRNA is induced in the *myostatin*-expressing C2C12 cells. When transfected with pSi-Mst, *p21* expression is down-regulated. (**d**) Western blot analysis of MyoD, a target gene of myostatin. MyoD is expressed in parental C2C12 cells, whereas it is not expressed in the *myostatin*-expressing C2C12 cells. When transfected with pSi-Mst, MyoD expression is retrieved. (**e**) Phase-contrast microscopic observation of the C2C12 cells. Multinuclear myotubes are observed in parental C2C12 cell (arrows), while not observed in the *myostatin*-expressing C2C12 cells. After inhibition of myostatin expression by transfection of pSi-Mst, multinuclear myotubes are retrieved (arrows). (**f**) Immunofluorescence of myosin heavy chain (MHC) in the C2C12 cells. MHC expression is observed in parental C2C12 cell, while not observed in the myostatin-expressing C2C12 cells. After inhibition of myostatin expression by transfection of pSi-Mst, MHC expression is retrieved.